

# Dissolution Rate Studies of Cholesterol Monohydrate in Bile Acid-Lecithin Solutions Using the Rotating-Disk Method

S. PRAKONGPAN, W. I. HIGUCHI, K. H. KWAN, and  
A. M. MOLOKHIA\*

**Abstract** □ A physical model approach was used to investigate cholesterol gallstone dissolution kinetics in simulated bile. Critical experimental and theoretical investigations simulating *in vivo* conditions showed that, in the bile acid-lecithin solutions, there is a significant interfacial barrier for both cholesterol gallstone and cholesterol monohydrate pellet dissolution. In the present study, the rotating-disk dissolution method and the accompanying Levich theory were applied to assess the contributions of the diffusion convection mass transfer resistance and of the interfacial barrier to the overall kinetics. Cholesterol dissolution rates in bile acid solutions were about 2–20 times slower than diffusion-controlled rates depending upon the degree of agitation. As found in previous studies, these rates in the presence of sufficient concentrations of dissolution accelerators approached the theoretical diffusion-convection-controlled rates. To account for the much slower dissolution rates in bile acid-lecithin solutions, two possible kinetic interpretations were investigated. The first is based upon slow crystal-micellar solution interfacial kinetics, and the second is based upon a slow rate of cholesterol solubilization in the aqueous diffusion layer. For the latter, an analytical mathematical solution was obtained.

**Keyphrases** □ Cholesterol monohydrate—dissolution rate studies in bile acid-lecithin solutions, rotating-disk method □ Bile acid-lecithin solutions—in cholesterol monohydrate dissolution rate studies, rotating-disk method □ Dissolution rate—cholesterol monohydrate in bile acid-lecithin solutions, rotating-disk method

Results of studies on the dissolution rate of human cholesterol gallstones and cholesterol monohydrate pellets in bile acid-lecithin solutions simulating bile were reported recently (1–4). An important finding was that there is a significant interfacial barrier for cholesterol gallstone and cholesterol monohydrate pellet dissolution in these bile-lecithin solutions. These studies also showed that when quaternary ammonium compounds were added to the solutions, the dissolution rates were enhanced dramatically and approached diffusion-controlled rates at sufficiently high concentrations.

These past studies involved experiments in which the gallstone and the cholesterol pellets were statically mounted in an assembly and solution agitation was accomplished by a paddle stirrer. The data were then analyzed by means of the conventional, semiempirical Nernst and Berthoud theories, involving the concept of an effective stagnant diffusion layer.

The purpose of the present report is to define more critically the baseline in bile acid-lecithin systems with and without the added dissolution rate accelerators. This approach is necessary for quantitative study of the structure-activity relationships for various medicinal agents capable of enhancing gallstone dissolution *in vivo*.

The rotating-disk method (5) and the accompanying Levich theory for analyzing the data are well

suited for quantifying the contributions of the diffusion-convection mass transfer resistance and of the interfacial barrier and/or the solubilization kinetics in the diffusion layer to the overall kinetics. Thus, this experiment-theory combination was chosen for these baseline studies. Together with other independent experiments, this approach has been able to establish quantitatively the limiting kinetic behavior for cholesterol in bile acid-lecithin solutions.

## THEORY

The dissolution process for a nonionic, nonreactive solid involves (a) the contact of the solvent with the solid interface, where (b) a physical reaction takes place. This reaction is followed by (c) the transport of the solute or products away from the interface into the bulk solution. In most cases of interest, since solvent contact occurs rapidly, steps (b) and/or (c) are generally considered to be rate determining.

The following discussion considers diffusion-controlled dissolution, interfacially controlled dissolution, and the situation when both may be important. An equation was derived (6) to account for both the interfacial resistance and the resistance for the transfer of the solute in solution from the vicinity of the solid surface into the bulk solvent under steady-state conditions:

$$\frac{dW}{dt} = J = \frac{A(C_s - C_b)}{h/D + 1/P} \quad (\text{Eq. 1})$$

where:

- $W$  = total amount of solid dissolved into solution at time  $t$
- $J$  = dissolution rate
- $A$  = surface area of solid exposed to solution
- $D$  = diffusion coefficient of solute in the solvent
- $C_s$  = saturated concentration of solute
- $C_b$  = concentration of solute in the bulk
- $P$  = effective interfacial permeability coefficient
- $h$  = Nernst effective diffusion layer thickness

When surface equilibrium is rapid,  $1/P$  is negligible and Eq. 1 becomes:

$$J = \frac{AD(C_s - C_b)}{h} \quad (\text{Eq. 2})$$

and the dissolution rate is determined by bulk transport only. When, on the other hand, equilibrium at the surface takes place slowly,  $1/P$  is much greater than  $h/D$  and:

$$J = AP(C_s - C_b) \quad (\text{Eq. 3})$$

Then the dissolution rate is determined by the rate of solute transfer at or near the solid-solution interface, and it is interfacially controlled.

In the context of the Nernst diffusion layer theory, the total resistance to solute transfer from the solution immediately adjacent to the solid surface into the bulk is given by  $h/D$ , a purely diffusional term. In most dissolution situations, both convection and diffusion are expected to be important. Therefore, for the rotating-disk case, the effective diffusional resistance,  $h/D$ , may be equated to an appropriate function which includes the consideration of both processes. Thus, for the rotating-disk situation in which only diffusion and convection are important, the mass flux was given by Levich (5) as:

$$J = 0.62AD^{2/3}\nu^{-1/6}\omega^{1/2}(C_s - C_b) \quad (\text{Eq. 4})$$

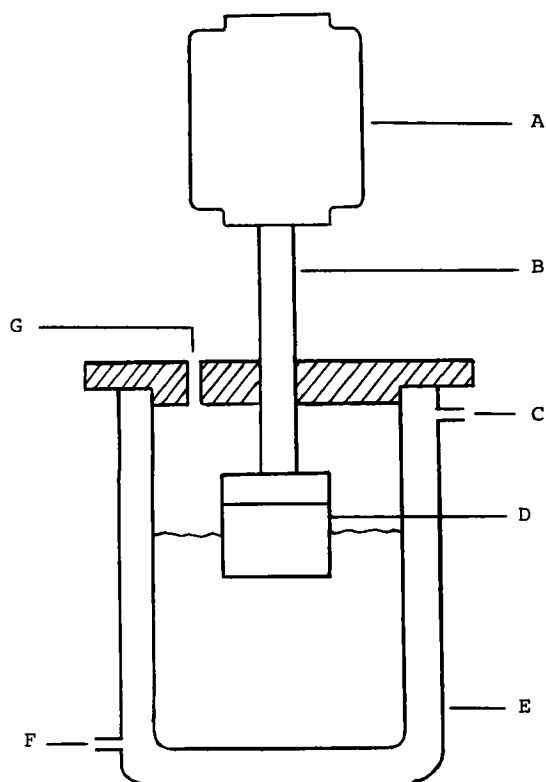


**Figure 1**—Rotating-disk apparatus for dissolution rate studies. Key: A, constant-speed motor; B, rotating shaft; C, water outlet; D, removable disk containing pellet; E, water-jacketed beaker; F, water inlet; and G, sample port.

where  $\nu$  is the kinematic viscosity, and  $\omega$  is the angular velocity of rotation.

The corresponding effective diffusion boundary layer thickness may be written as:

$$h = 1.612D^{1/3}\nu^{1/6}\omega^{-1/2} \quad (\text{Eq. 5})$$

A closer approximation for the rotating-disk problem by Gregory and Riddiford (7) gives:

$$h = 1.805[0.8934 + 0.316(D/\nu)^{0.36}]D^{1/3}\nu^{1/6}\omega^{-1/2} \quad (\text{Eq. 6})$$

Use of this value of  $h$  gives a 3% smaller theoretical dissolution rate than that predicted by Eq. 4 for  $D/\nu \approx 10^{-3}$ .

In a purely bulk transport-controlled case, the observed dissolution rate should be essentially equal to the calculated flux (Eq. 4). If, however, the observed reaction rate is substantially lower than the calculated diffusion-convection flux, it may be concluded that the dissolution process is taking place in the interfacially controlled region.

## EXPERIMENTAL

**Materials**—Sodium cholate<sup>1</sup> was used as received after the purity was checked with TLC. Recrystallized <sup>14</sup>C-labeled cholesterol monohydrate was prepared as previously described (3). A pure grade of egg lecithin was prepared using the method of Singleton *et al.* (8). The product was examined by TLC and shown to have very high purity.

**Solubility and Diffusion Coefficient Determination**—The methods described previously (3) were applied in this study.

**Dissolution Rate Determination**—Figure 1 is a schematic representation of the rotating-disk dissolution apparatus. It consists of three main parts: the outside water-jacketed beaker maintained at 37 ± 0.02°, the removable disk assembly, and the controlled-rotating device<sup>2</sup>. Figure 2 shows a schematic outline of the rotating disk with a pellet of the material under investigation mounted in place.

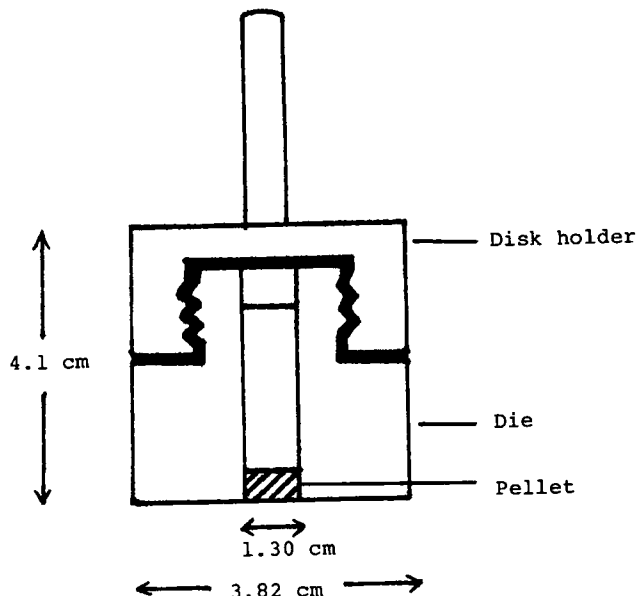


**Figure 2**—Cross-section of removable disk assembly with pellet.

Pellets of radioactive cholesterol monohydrate or benzoic acid were prepared by directly compressing 100 mg of the material in a die, 1.3 cm (0.5 in.) i.d., under a force of 1362 kg (3000 lb) using a laboratory press<sup>3</sup>. The die with the pellet was then firmly attached to the disk holder (Fig. 2).

For each dissolution run, 100 ml of solvent was pipetted into the beaker (Fig. 1). The rotating disk containing the pellet was then centered at about 1 cm below the solvent level so that the distances from the disk wall to the inner surface of the beaker exceeded 0.5 cm [these dimensions were shown (7) to provide adequate hydrodynamics within the system]. At the moment of contact between the pellet and the solvent, the motor and a timer were started simultaneously. Samples were withdrawn from the system by pipet at suitable time intervals for analysis in a liquid scintillation counter<sup>4</sup>.

The rotational speeds tested varied from 20 to 600 rpm, corresponding to Reynolds numbers of 1100 and 32,600, respectively.

Benzoic acid was used as a model solute compound for assessing the geometry effects and the hydrodynamics within the system because benzoic acid has been known to dissolve by diffusion-convection control.

## RESULTS AND DISCUSSION

**Dissolution of Benzoic Acid**—The results of the dissolution experiments of benzoic acid in 0.01 *N* hydrochloric acid are presented in Figs. 3 and 4. Figure 3 shows the relation between the amounts dissolved and time. The linear plots were obtained at all speeds of rotation, indicating constant rates during the time of each run.

When these dissolution rates were plotted *versus* the square root of the speed of rotation (Fig. 4), a linear relationship was obtained and was compared to the dissolution rates predicted by the Levich (5) theory (Eq. 4). However, the experimental rates were found to be about 14% lower than those predicted by the theory. This discrepancy is consistent with Riddiford's (9) views regarding the performance of rotating-disk geometries of the type used in the present study.

The benzoic acid data clearly show that diffusion-convection is the sole limiting step in the dissolution of benzoic acid in these experiments. The linear dependency of the dissolution rate  $J$  on  $\omega^{1/2}$ , even at high speeds of rotation, indicates that a fast equilibrium is taking place at the pellet surface.

**Dissolution of <sup>14</sup>C-Cholesterol Monohydrate**—Table I summarizes the experimental cholesterol monohydrate dissolution rate data together with the solubilities and diffusion coefficients in 2%

<sup>1</sup> Schwarz/Mann, Orangeburg, N.Y.

<sup>2</sup> Servodyne laboratory stirrer, Cole-Parmer Instrument Co., Chicago, Ill.

<sup>3</sup> Model B, Fred Carver, Inc., Summit, N.J.

<sup>4</sup> Beckman Instruments Inc., Fullerton, Calif.

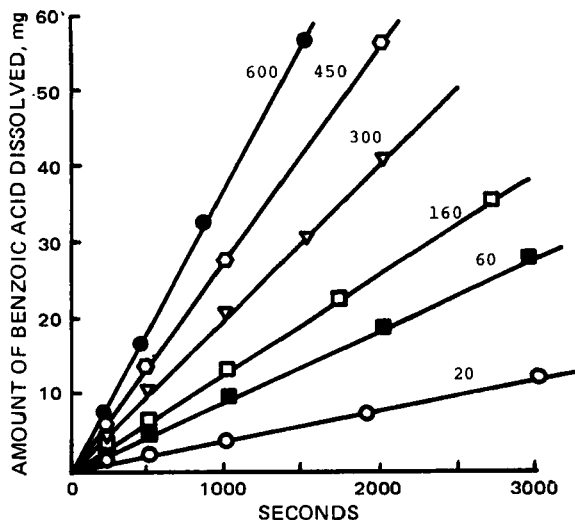


Figure 3—Dissolution of benzoic acid pellets ( $A = 1.27 \text{ cm}^2$ ) into  $0.01 \text{ N HCl}$  at various rotational speeds. Numbers on line refer to rotational speeds (revolutions per minute).

bile acid and 2% bile acid–1% lecithin media with and without benzalkonium chloride.

To present the data in a more meaningful way, Eq. 4 was rearranged to:

$$J/0.62AD^{2/3}\nu^{-1/6}C_s = \omega^{1/2} \quad (\text{Eq. 7})$$

so that, for a diffusion-controlled dissolution, a plot of the left-hand side versus the right-hand side should give a straight line with a slope of unity. The presence of a significantly slow interfacial step should result in a significant negative deviation from linearity, and these deviations should increase with increasing  $\omega^{1/2}$ .

Figure 5 shows the cholesterol monohydrate dissolution rate data plotted according to Eq. 7. In the sodium cholate–lecithin solution (Table I and Fig. 5), the dissolution rates were essentially unaffected by changes in the rotation speeds; the results were close to those determined by the static pellet dissolution method (3). Thus, the interfacial resistance plays the dominant role as the rate-determining step in cholesterol monohydrate dissolution in synthetic bile, even at very low agitation.

Addition of benzalkonium chloride to the bile acid–lecithin system increased the rate of cholesterol monohydrate dissolution, as was found previously (4). As the concentration of benzalkonium

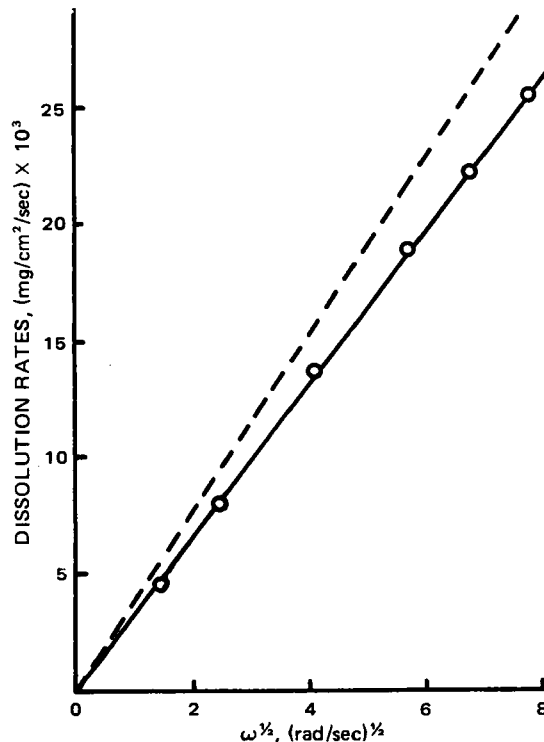


Figure 4—Comparison between observed and predicted effects of stirring speed on the dissolution rate of a benzoic acid pellet in  $0.01 \text{ N HCl}$  at  $37^\circ$ . Key: —○—, observed; and - - -, predicted by Eq. 4.

chloride was varied from 0.25 to 2%, the dissolution behavior gradually changed from being largely interfacially controlled to being essentially diffusion controlled and quantitatively predicted by the Levich theory and the benzoic acid dissolution data (Table I and Fig. 5).

Table II presents the effective permeability coefficients ( $P$ ) for systems showing considerable interfacial resistance to cholesterol monohydrate dissolution. These values were calculated from the experimental rates using:

$$J' = \frac{A(C_s - C_b)}{1.612D^{-2/3}\nu^{1/6}\omega^{-1/2} + 1/P} \quad (\text{Eq. 8})$$

Table I—Dissolution Rates ( $J$ ), Solubilities ( $C_s$ ), and Diffusivities ( $D$ ) of Cholesterol Monohydrate in Test Solutions

Solvent Media <sup>a</sup>			$C_s$ , mg/ml	$D \times 10^6$ , cm <sup>2</sup> /sec	$J \times 10^4$ , mg/cm <sup>2</sup> /sec			
C, %	L, %	BC, %			20 rpm	60 rpm	300 rpm	600 rpm
2	—	—	0.53	2.17	0.23	0.26	0.33	0.39
2	1	—	1.05	1.491	0.11	0.13	0.15	0.16
2	1	0.25	1.20	1.30	1.05	1.62	2.20	2.37
2	1	0.50	1.55	1.30	2.74	4.60	8.12	9.01
2	1	1.0	2.20	1.29	3.61	6.14	11.2	15.7
2	1	2.0	3.30	1.40	4.82	9.87	22.4	29.6

<sup>a</sup> In  $0.1 \text{ M}$  phosphate buffer, pH 7.4. C = sodium cholate, L = lecithin, and BC = benzalkonium chloride.

Table II—Permeability Coefficient ( $P$ ) of Cholesterol Monohydrate in Test Solutions

Solvent Media <sup>a</sup>			$P \times 10^4$ , cm/sec				Mean $\pm$ SD <sup>b</sup>
C, %	L, %	BC, %	20 rpm	60 rpm	300 rpm	600 rpm	
2	—	—	0.54	0.54	0.66	0.77	0.656 $\pm$ 0.013
2	1	—	0.11	0.13	0.15	0.15	0.143 $\pm$ 0.001
2	1	0.25	1.50	2.14	2.35	2.38	2.29 $\pm$ 0.02
2	1	0.50	11.0	16.0	14.7	11.7	14.1 $\pm$ 2.2
2	1	1.0	8.19	13.0	14.2	19.6	15.6 $\pm$ 3.5

<sup>a</sup> In  $0.1 \text{ M}$  phosphate buffer, pH 7.4. C = sodium cholate, L = lecithin, and BC = benzalkonium chloride. <sup>b</sup> The value at 20 rpm is not included.

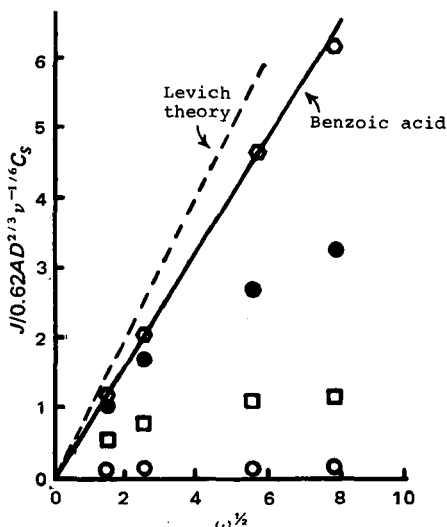


**Figure 5**—Dissolution rates of cholesterol monohydrate in: O, 2% sodium cholate + 1% lecithin; □, 2% sodium cholate + 1% lecithin + 0.25% benzalkonium chloride; ●, 2% sodium cholate + 1% lecithin + 0.5% benzalkonium chloride; and ○, 2% sodium cholate + 1% lecithin + 2% benzalkonium chloride in 0.1 M phosphate buffer, pH 7.4.

Equation 8 is obtained by substituting Eq. 5 into Eq. 1;  $J'$  refers to the corrected rate (based upon the benzoic acid data). Except at 20 rpm, the  $P$  values were essentially constant for each system. When the average  $P$  values were used to generate theoretical dissolution rates of cholesterol monohydrate, a good fit with the experimental rates was observed (Fig. 6).

**Possible Physical Meaning of  $P$** —The permeability coefficient,  $P$ , may be shown to be associated with transfer kinetics at the crystal-solution interface or solubilization kinetics in the diffusion layer or both. When slow cholesterol transfer occurs at the cholesterol monohydrate crystal-solution interface,  $P$  may be considered to be a first-order reaction rate constant associated with this rate-determining process (1). If the process involves the slow solubilization of the aqueous free cholesterol by the micelles in the diffusion layer,  $P$  has an entirely different meaning.

The theoretical treatment for the latter case is presented in the Appendix, where it is shown that the two situations may have identical mathematical form from the hydrodynamic standpoint and may be considered to be mathematically equivalent if:

$$P = \frac{\sqrt{k_f D_f}}{K} \quad (\text{Eq. 9})$$

where  $k_f$  is the forward reaction rate constant,  $D_f$  is the diffusion coefficient of free cholesterol, and  $K$  is the equilibrium constant.

While more definitive experiments may be necessary before it can be determined which of the two mechanisms is more likely to be correct, the collective evidence strongly supports the crystal-solution interfacial reaction mechanism. One argument is that the mechanism based upon slow solubilization in the diffusion layer predicts that  $P$  would be proportional to the reciprocal of the square root of the micelle concentration. This can be seen from Eq. 9 since both  $k_f$  and  $K$  would be expected to be approximately proportional to the micelle concentration.

Other studies (2, 10) have shown, however, that at high ionic strength,  $P$  is either nearly constant or increases somewhat with increasing micelle concentrations over a 1–5% sodium cholate concentration range. Therefore, these data support the mechanism in which the slow step is kinetics at the crystal-solution interface and not the kinetics of cholesterol solubilization in the aqueous diffusion layer.

Other evidence supporting this viewpoint is that  $P$  has been found to be sensitive to electrolytes. Current studies in these laboratories indicate that  $P$  increases about fivefold when the phosphate buffer concentration is increased from 0.01 to 0.1 M. Also Surpuriya and Higuchi (10, 11) found similar electrolyte effects in their kinetic studies on the oil-water transport of cholesterol. These results are consistent with a micelle-interface interaction mechanism in which the close approach of a negatively charged

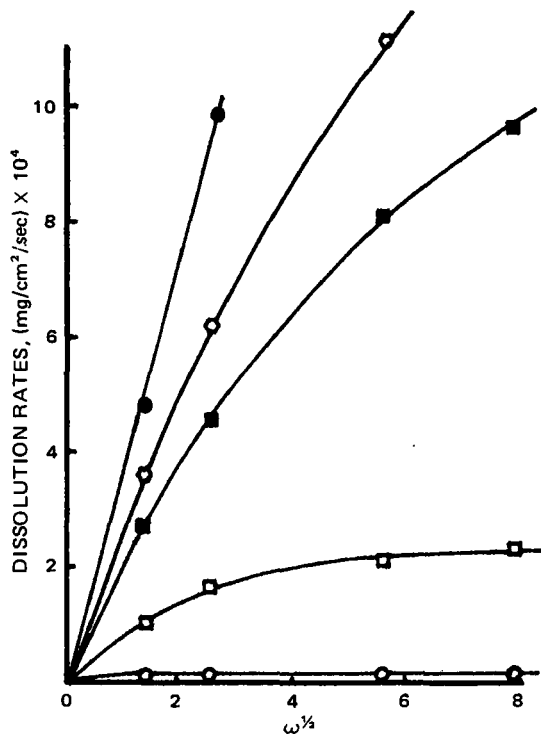
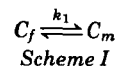


**Figure 6**—Comparison of the theoretical (solid line) dissolution rates using average  $P$  values (Table II) with the experimental dissolution rates for cholesterol monohydrate pellets in: O, 2% sodium cholate + 1% lecithin; □, 2% sodium cholate + 1% lecithin + 0.25% benzalkonium chloride; ■, 2% sodium cholate + 1% lecithin + 0.5% benzalkonium chloride; ○, 2% sodium cholate + 1% lecithin + 1% benzalkonium chloride; and ●, 2% sodium cholate + 1% lecithin + 2% benzalkonium chloride.

micelle to a negatively charged surface is facilitated by counterions or by increasing ionic strength in general. Also, the strong influence of benzalkonium chloride upon  $P$  appears to be more consistent with a mechanism involving the interface than one involving micellar kinetics in the aqueous diffusion layer.

## APPENDIX

The dissolution rate equation for nonequilibrium reaction kinetics in the diffusion layer is derived as follows. The reaction of cholesterol with the bile acid-lecithin micelles is given as:



and:

$$K = \frac{k_f}{k_r} \quad (\text{Eq. A1})$$

where:

- $C_f$  = concentration of free cholesterol
- $C_m$  = concentration of micellar cholesterol
- $k_f$  = forward reaction rate constant
- $k_r$  = reverse reaction rate constant
- $K$  = equilibrium constant

The steady-state diffusion equations for free and micellar cholesterol in the region  $0 \leq x \leq h$  (the diffusion layer thickness) are:

$$D_f \frac{d^2 C_f}{dx^2} - k_f \left( C_f - \frac{C_m}{K} \right) = 0 \quad (\text{Eq. A2})$$

$$D_m \frac{d^2 C_m}{dx^2} + k_f \left( C_f - \frac{C_m}{K} \right) = 0 \quad (\text{Eq. A3})$$

where  $D_f$  is the diffusion coefficient of free cholesterol, and  $D_m$  is the diffusion coefficient of micellar cholesterol.

The boundary conditions at  $x = 0$  are  $C_f = C_f^0$ ,  $C_m = C_m^0$ , and  $(dC_m/dx) = 0$ . At  $x = h$ ,  $C_f = 0$  and  $C_m = 0$ .

Combining Eqs. A2 and A3 and integrating with these boundary conditions give:

$$C_f = \frac{D_m}{D_f} C_m + \left( C_f^0 + \frac{D_m C_m^0}{D_f} \right) \left( 1 - \frac{x}{h} \right) \quad (\text{Eq. A4})$$

for  $(0 \leq x \leq h)$ .

Substituting Eq. A4 into Eq. A3 and rearranging give:

$$\frac{d^2 C_m}{dx^2} - \frac{k_f}{D_m} \left( \frac{D_m}{D_f} + \frac{1}{k} \right) C_m = - \frac{k_f}{D_m} \left( C_f^0 + \frac{D_m C_m^0}{D_f} \right) \left( 1 - \frac{x}{h} \right) \quad (\text{Eq. A5})$$

Equation A5 can be solved analytically for  $C_m$  to give:

$$C_m = \left[ C_m^0 - \left( \frac{D_f C_f^0 + D_m C_m^0}{B_m + D_f/K} \right) \left( \frac{e^{x\sqrt{A}} - e^{-x\sqrt{A}}}{1 - e^{2h\sqrt{A}}} \right) \right] - \left( \frac{D_f C_f^0 + D_m C_m^0}{D_m + D_f/K} \right) \left( 1 - \frac{x}{h} \right) \quad (\text{Eq. A6})$$

where:

$$A = \left( \frac{k_f}{D_f} + \frac{k_f}{D_m K} \right) \quad (\text{Eq. A7})$$

By differentiating Eq. A6 with  $(dC_m/dx)_{x=0} = 0$ ,  $C_m^0$  can be obtained algebraically:

$$C_m^0 = \frac{\frac{D_f C_f^0}{D_m + D_f/K} \left[ 1 + \frac{(1 - e^{2h\sqrt{A}})}{h\sqrt{A}(1 + e^{2h\sqrt{A}})} \right]}{1 - \left( \frac{D_m}{D_m + D_f/K} \right) \left( 1 + \frac{(1 - e^{2h\sqrt{A}})}{h\sqrt{A}(1 + e^{2h\sqrt{A}})} \right)} \quad (\text{Eq. A8})$$

The total diffusional flux of cholesterol is:

$$J = \frac{D_m C_m^0}{h} + \frac{D_f C_f^0}{h} \quad (\text{Eq. A9})$$

and the flux from free cholesterol ( $D_f C_f^0/h$ ) can be neglected in this case. Substituting Eq. A8 into Eq. A9 and rearranging give:

$$J = \frac{D_m C_f^0}{h} \left[ \frac{(1 - e^{2h\sqrt{A}}) + h\sqrt{A}(1 + e^{2h\sqrt{A}})}{\frac{h\sqrt{A}}{K}(1 + e^{2h\sqrt{A}}) - \frac{D_m}{D_f}(1 - e^{2h\sqrt{A}})} \right] \quad (\text{Eq. A10})$$

For  $h\sqrt{A} \gg 1$ , Eq. A10 can be reduced to:

$$J = \frac{K C_f^0}{\frac{h}{D_m} + \sqrt{k_f D_f}} \quad (\text{Eq. A11})$$

## REFERENCES

- (1) W. I. Higuchi, S. Prakongpan, V. Surpuriya, and F. Young, *Science*, **178**, 633(1972).
- (2) W. I. Higuchi, V. Surpuriya, S. Prakongpan, and F. Young, *J. Pharm. Sci.*, **62**, 695(1973).
- (3) W. I. Higuchi, S. Prakongpan, and F. Young, *ibid.*, **62**, 945(1973).
- (4) *Ibid.*, **62**, 1207(1973).
- (5) V. G. Levich, "Physicochemical Hydrodynamics," Prentice-Hall, Englewood Cliffs, N.J., 1962.
- (6) A. Berthoud, *J. Chem. Phys.*, **10**, 624(1912).
- (7) D. P. Gregory and A. C. Riddiford, *J. Chem. Soc.*, **1956**, 3756.
- (8) W. S. Singleton, M. S. Gray, M. L. Brown, and J. L. White, *J. Amer. Oil Chem. Soc.*, **42**, 53(1965).
- (9) A. C. Riddiford, in "Advances in Electrochemistry and Electrochemical Engineering," vol. 4, P. Delahay, Ed., Interscience, New York, N.Y., 1966, p. 47.
- (10) V. Surpuriya and W. I. Higuchi, *J. Pharm. Sci.*, **61**, 375(1972).
- (11) V. Surpuriya and W. I. Higuchi, *Biochim. Biophys. Acta*, **290**, 375(1972).

## ACKNOWLEDGMENTS AND ADDRESSES

Received May 9, 1975, from the College of Pharmacy, University of Michigan, Ann Arbor, MI 48104

Accepted for publication July 16, 1975.

Supported by the National Institute of Arthritis, Metabolism and Digestive Diseases (Grant AM 16694).

The authors thank Dr. J. S. Schultz for help in developing the theory for the kinetics of solubilization in the diffusion layer.

\* To whom inquiries should be directed.

## Chlorpromazine Metabolism VII: New Quantitative Fluorometric Determination of Chlorpromazine and Its Sulfoxide

PUSHKAR N. KAUL<sup>\*</sup>, LLOYD R. WHITFIELD, and MERVIN L. CLARK

**Abstract** □ A new, sensitive assay is described for chlorpromazine and/or its sulfoxide. The method is based on reacting the tertiary amine base with 9-bromomethylacridine to form a quaternary compound which, on photolysis, yields highly fluorescent products that are determinable fluorometrically. The procedural steps were standardized, and an optimum assay procedure was developed. The method shows a less than 3% coefficient of variation when applied directly to chlorpromazine samples and is capable of determining 15–20 ng of the drug. The method is readily adaptable to clinical and bioavailability studies.

**Keyphrases** □ Chlorpromazine and its sulfoxide—fluorometric analysis after quaternization with 9-bromomethylacridine, pharmaceutical formulations and blood levels □ 9-Bromomethylacridine—quaternization reagent for fluorometric analysis of chlorpromazine and its sulfoxide, pharmaceutical formulations and blood levels □ Fluorometry—analysis, chlorpromazine and its sulfoxide, pharmaceutical formulations and blood levels □ Tranquilizers—chlorpromazine, fluorometric analysis, pharmaceutical formulations and blood levels

Of the many assay methods (1–12) developed for chlorpromazine, those possessing adequate sensitivity to determine its levels in blood include a GC method and its modifications (2, 3, 5), *in vitro* radioassay (6), radioimmunoassay (9, 10), and GC–mass spec-

troscopy (4). The lack of precision in GC methods has been adequately reiterated (11–13). The *in vitro* radioquantitation method has not been applied successfully, perhaps because of its complicated nature and poor precision. A reported radioimmunoassay (9)